Study of the Reaction $\pi^+ + p \rightarrow \Sigma^+ + K^+$ near Threshold*

FERNAND GRARD† AND GERALD A. SMITH
Lawrence Radiation Laboratory, University of California, Berkeley, California
(Received March 9, 1962)

The reaction $\pi^+ + p \rightarrow \Sigma^+ + K^+$ has been studied in the momentum range 1037 through 1065 MeV/c with specific regard to the determination of s- and p-wave amplitudes. If we represent these amplitudes near threshold by $S_{\frac{1}{2}} = a_0 k^{\frac{1}{2}}$, $P_{\frac{1}{2}} + 2P_{\frac{3}{2}} = b_0 k^{\frac{3}{2}} e^{i\chi_b}$, and $P_{\frac{1}{2}} - P_{\frac{3}{2}} = c_0 k^{\frac{3}{2}} e^{i\chi_c}$, the following results have been obtained from an analysis based on 274 events: $a_0^2 = (3.31 \pm 0.87) \times 10^{-5}$ mb/sr-MeV/c, $b_0/a_0 = 0.0075 \pm 0.0026$, $c_0/a_0 = -0.0062 \pm 0.0023$, $\chi_b = 52.1 \pm 8.0$ deg, $\chi_c = 80.8 \pm 27.2$ deg. An alternative set of solutions exists for $\chi_b = -52.1$ deg and $\chi_c = 99.2$ deg.

I. INTRODUCTION

THE reaction $\pi^+ + p \rightarrow \Sigma^+ + K^+$ has been studied near the threshold (1020 MeV/c) in the 72-in. liquid hydrogen bubble chamber. Energy loss in the incident beam by ionization in the hydrogen has permitted an analysis of the reaction in the momentum interval 1037 through 1065 MeV/c. Several other workers have analyzed this reaction at higher momenta in bubble chambers[1–5]; one experiment has been done in this low-energy range.[5] However, since only five events were reported, a detailed analysis of $\Sigma^+ K^+$ threshold properties was impossible. In this paper, 274 events have been analyzed with specific regard to a partial-wave determination of the reaction near threshold. From the distribution of events as a function of incident pion momentum, c.m. production angle, Σ^+-decay angle with respect to the normal to production plane, and total cross section, the s- and p-wave production amplitudes have been determined from the data. Based on an extrapolation of these results to 1090 MeV/c, an attempt to check the charge-independence hypothesis has been made with currently available data of Σ^- and Σ^0 production by π^-, p interaction.[6,7]

II. EXPERIMENTAL DETAILS

The experimental beam setup has been described previously.[8] In addition to the beam optics shown in Fig. 1 of reference 8, a quadrupole lens and a mass spectrometer were used to produce a separated π^+ beam. The momentum resolution of the beam was $(^{+2.2}_{-4.0})$ MeV/c, the same as that given for π^- in Fig. 3 of reference 8. The incident π^+ beam was of such momentum that by energy degrading in the liquid hydrogen, the threshold for $\Sigma^+ K^+$ was placed in the vicinity of the downstream end of the bubble chamber. A determination of the threshold would then allow a very accurate measure of the incident beam momentum.

In order to estimate the proton contamination in the beam, a sample of two-prong interactions was analyzed for elastic pion-proton and proton-proton scatterings. The cross sections for these reactions were taken to be 10.3 ± 0.9 and 25.0 ± 1.0 mb, respectively, at 1040 MeV/c.[9,10] Proton contamination was measured to be $4.9 \pm 2.0\%$.

Positron and muon contamination was measured from bremsstrahlung and δ-ray production in the chamber. The principle of this determination was the following. The energies of the δ rays and the secondary track in bremsstrahlung events were measured on the scanning table by means of curvature templates, the δ rays being counted in two momentum intervals: from 53 through 90 MeV/c, and from 90 through 1060 MeV/c. Since the upper limits of the δ-ray spectrum are 53 MeV/c when produced by 1060-MeV/c pions, and 90 MeV/c in the case of 1060-MeV/c muons, the δ rays selected in the first interval were produced by either positrons or muons. The corresponding absolute cross sections estimated by integration over this momentum interval are equal to 1.85 and 0.48 mb respectively.[11] The δ rays selected in the second energy interval were unambiguously produced by positrons. The integrated cross section is 1.99 mb.[11] The bremsstrahlung events were selected for secondary track momentum less than 500 MeV/c, to avoid possible confusion with incident pions decaying in the chamber

* This work was done under the auspices of the U. S. Atomic Energy Commission.
† On leave from the Institut Interuniversitaire des Sciences Nucléaires, Belgium.
[1] J. L. Brown, D. A. Glaser, D. I. Meyer, M. L. Perl, and J. Vander Velde, Phys. Rev. **107**, 906 (1957).
[2] A. R. Erwin, Jr., J. K. Kopp, and A. M. Shapiro, Phys. Rev. **115**, 669 (1959).
[3] W. H. Hannum, H. Courant, E. C. Fowler, H. L. Kraybill, J. Sandweiss, and J. Sanford, Phys. Rev. **118**, 577 (1960).
[4] A. Berthelot, A. Daudin, O. Goussu, F. Grard, M.-A. Jabiol, F. Levy, C. Lewin, A. Rogozinski, J. Laberrigue-Frolow, C. Ouannes, and L. Vigneron, Nuovo cimento **21**, No. 5, 693 (1961).
[5] C. Baltay, H. Courant, W. J. Fickinger, E. C. Fowler, H. L. Kraybill, J. Sandweiss, J. R. Sanford, D. L. Stonehill, and H. D. Taft, Revs. Modern Phys. **33**, 374.
[6] F. Eisler, R. Plano, A. Prodell, N. Samios, M. Schwartz, J. Steinberger, P. Bassi, V. Borelli, G. Puppi, H. Tanaka, P. Waloschek, V. Zoboli, M. Conversi, P. Franzini, I. Mannelli, R. Santangelo, and V. Silvestrini, Nuovo cimento **10**, No. 3, 468 (1958).
[7] Frank S. Crawford, Jr. (private communication).
[8] S. E. Wolf, N. Schmitz, L. J. Lloyd, W. Laskar, F. S. Crawford, Jr., J. Button, J. A. Anderson, and G. Alexander, Revs. Modern Phys. **33**, 439 (1961).
[9] D. Stonehill, C. Baltay, H. Courant, W. Fickinger, E. C. Fowler, H. Kraybill, J. Sandweiss, J. Sanford, and H. Taft, Phys. Rev. Letters **6**, 624 (1961).
[10] S. J. Lindenbaum, Ann. Rev. Nuclear Sci. **7**, 317 (1957).
[11] H. I. Bhabha, Proc. Roy. Soc. (London), **A164**, 257 (1938); B. Rossi, *High-Energy Particles* (Prentice-Hall, Inc., Englewood Cliffs, New Jersey, 1952).

into muons (the lower limit of the muon spectrum in the laboratory system is about 610 MeV/c; in addition, scanning efficiency is optimum for these events). The absolute cross section estimated by integration from zero momentum up to 500 MeV/c is equal to 8.70 mb for incident positrons of 1060 MeV/c slowed down in the field of hydrogen nuclei.[12] Positron contamination was measured to be $(1.3\pm0.4)\%$, and the muon contamination to be $(0.5\pm0.5)\%$. The combined proton, positron, and muon contamination was $(6.7\pm2.5)\%$.

A total of 105 000 pictures was scanned for Σ^+K^+ events, and approximately 20% of these were rescanned. Events were measured on the Franckenstein measuring machines at the Lawrence Radiation Laboratory (Berkeley). During this experiment the magnetic field in the chamber was 15.7 kG. Events were reconstructed and analyzed kinematically by means of the programs PANG and KICK,[13] the latter program providing fitted angles and momenta that were introduced to subsequent detailed analysis programs.

III. PARTIAL-WAVE ANALYSIS OF Σ^+K^+ NEAR THRESHOLD

Preliminary analysis[14] of events indicated large asymmetries in the c.m. production angular distribution and the up-down decay distribution of the Σ^+ in the mode $\Sigma^+\rightarrow p+\pi^0$. This information implied the presence of at least p wave in the production mechanism. The experimental data showed no evidence for a significant amount of d wave.

Assuming only s and p waves at the production of Σ^+K^+, the angular distribution $d\sigma/d\Omega$ and polarization P can be written

$$d\sigma/d\Omega=A_0+A_1\cos\theta+A_2\cos^2\theta, \tag{1-A}$$

and

$$P(d\sigma/d\Omega)=\sin\theta(A_3+A_4\cos\theta). \tag{1-B}$$

Assume that the Σ^+ is created at an angle θ in the production c.m. system, and decays into a pion making an angle ϕ with respect to the normal

$$n=\mathbf{P}_\pi\times\mathbf{P}_\Sigma/|P_\pi||P_\Sigma|\sin\theta_{\pi\Sigma}$$

to the production plane in the Σ^+ rest frame. Then the probability function for the observation of an event is

$$f=A_0+A_1\cos\theta+A_2\cos^2\theta +\alpha\cos\phi\sin\theta(A_3+A_4\cos\theta), \tag{2}$$

where use has been made of the fact that the Σ^+ parity-nonconserving decay distribution of the pion is of the form $(1+\alpha P\cos\phi)$. The α is the asymmetry parameter for the Σ^+ decay (α^+ for $n\pi^+$, and α^0 for $p\pi^0$). Near threshold, the coefficients of Eq. (2), according to Lee *et al.*,[15] would be

$$\begin{aligned}A_0&=a_0^2k+c_0^2k^3,\\ A_1&=2a_0b_0k^2\cos\chi_b,\\ A_2&=(b_0^2-c_0^2)k^3,\\ A_3&=-2a_0c_0k^2\sin\chi_c,\end{aligned} \tag{3}$$

and

$$A_4=2b_0c_0k^3\sin(\chi_b-\chi_c),$$

where k is the Σ^+ momentum in the production c.m. and the parameters a_0, b_0, c_0, χ_b, χ_c, are related to the $S_{1/2}$, $P_{1/2}$, and $P_{3/2}$ production amplitudes by

$$\begin{aligned}S_{1/2}&=a_0k^{\frac{1}{2}},\\ P_{1/2}+2P_{3/2}&=b_0k^{\frac{3}{2}}e^{i\chi_b},\\ P_{3/2}-P_{1/2}&=c_0k^{\frac{3}{2}}e^{i\chi_c}.\end{aligned} \tag{4}$$

The s- and p-wave amplitudes have been determined by the maximum-likelihood method, assuming that the energy dependence of Eq. (3) is still valid in the energy range investigated. The probability function may be written as

$$f=X_0k+X_1k^3+X_2k^2\cos\theta+X_3k^3\cos^2\theta +X_4\cos\phi\sin\theta k^2+X_5\cos\phi\sin\theta\cos\theta k^3, \tag{5}$$

where

$$\begin{aligned}X_0&=a_0^2,\\ X_1&=c_0^2,\\ X_2&=2a_0b_0\cos\chi_b,\\ X_3&=b_0^2-c_0^2,\\ X_4&=-2\alpha a_0c_0\sin\chi_c,\\ X_5&=-2\alpha b_0c_0\sin(\chi_c-\chi_b).\end{aligned}$$

Near threshold, k is related to the incident pion momentum p, by

$$k(\mathrm{MeV}/c)=r(p-1020\ \mathrm{MeV}/c)^{\frac{1}{2}}=r(\Delta p)^{\frac{1}{2}}, \tag{6}$$

where

$$r=\left\{\frac{0.991m_p}{2}\left[1-\frac{(m_K^2-m_\Sigma^2)^2}{(m_K+m_\Sigma)^4}\right]\right\}^{\frac{1}{2}}=19.63(\mathrm{MeV}/c)^{\frac{1}{2}}. \tag{7}$$

The probability function, Eq. (5), may now be written in terms of the laboratory-system momentum p,

$$f=Y_0(\Delta p)^{\frac{1}{2}}+Y_1(\Delta p)^{\frac{3}{2}}+Y_2\cos\theta(\Delta p)+Y_3\cos^2\theta(\Delta p)^{\frac{3}{2}} +Y_4\cos\phi\sin\theta(\Delta p)+Y_5\cos\phi\sin\theta\cos\theta(\Delta p)^{\frac{3}{2}}, \tag{8}$$

[12] W. Heitler, *The Quantum Theory of Radiation* (Oxford University Press, New York, 1954), 3rd ed.; H. Bethe, Proc. Cambridge Phil. Soc. **30**, 524, 1934.

[13] A. H. Rosenfeld, in *Proceedings of the International Conference on High-Energy Accelerators and Instrumentation, CERN, 1959* (CERN Scientific Information Service, Geneva, 1959), pp. 533–541; W. E. Humphrey, "A Description of the PANG program," Alvarez Group Memos No. 111 and 115, Lawrence Radiation Laboratory, Berkeley (unpublished); J. P. Berge, F. T. Solmitz, and H. Taft, Rev. Sci. Instr. **32**, 538 (1961).

[14] F. Grard and G. A. Smith, Bull. Am. Phys. Soc., **7**, 48 (1962).

[15] T. D. Lee, J. Steinberger, G. Feinberg, P. K. Kabir, and C. N. Yang, Phys. Rev. **106**, 1367 (1957).

where

$$Y_0 = a_0^2 r,$$
$$Y_1 = c_0^2 r^3,$$
$$Y_2 = 2a_0 b_0 r^2 \cos\chi_b,$$
$$Y_3 = (b_0^2 - c_0^2) r^3,$$
$$Y_4 = -2\alpha a_0 c_0 r^2 \sin\chi_c,$$

and

$$Y_5 = -2\alpha b_0 c_0 r^3 \sin(\chi_c - \chi_b).$$

For each event the values of $\cos\theta$ and $\cos\phi$, and the y coordinate of the production vertex in the chamber are known. The y axis is directed along the 72-in. dimension of the chamber, with the center of the chamber at $y=0$ cm. Δp is related to $\Delta y = y_{\rm th} - y$, where $y_{\rm th}$ is the coordinate of the threshold, by $\Delta p(\mathrm{MeV}/c) = 0.243\Delta y$ (cm). The curvature of the tracks over the whole length of the chamber introduces no significant deviation from this formula ($<0.5\%$). For a given y coordinate there is a corresponding most likely value of the incident momentum $\bar{p}$, around which the real value $p = \bar{p} + \epsilon$ fluctuates, according to the resolution curve $f(\epsilon)$ of Fig. 3 in reference 8. Therefore, the probability function has been folded in with the momentum resolution curve (normalized to unity). The quantities $(\Delta p)^n$ in Eq. (8) have been replaced by

$$\langle \Delta p^n \rangle_{\rm av} = \int_{0.243(y-y_{\rm th})}^{y_{\rm max}} d\epsilon\, f(\epsilon)[0.243(y_{\rm th}-y)+\epsilon]^n. \quad (9)$$

To construct the likelihood function the probability density,

$$\mathcal{P} = \frac{f \exp[-(y-y_{\rm min})/\lambda]}{\int_{-1}^{+1} d(\cos\phi) \int_a^b d(\cos\theta) \int_{y_{\rm min}}^{y_{\rm max}} f \exp[-(y-y_{\rm min})/\lambda] dy}, \quad (10)$$

is required. The exponential factor takes into account the beam attenuation by all strong interactions with a total mean free path λ (1.16×10^3 cm).[9] The integrations extend over the whole range of physical quantities in which the experimental results are given. Provision has been made for cutting the production angular distribution in the forward and backward directions. In order to find the best values of the parameters a_0, b_0, c_0, χ_b, χ_c, the likelihood function

$$\mathcal{L} = \prod_{i=1}^{N} \mathcal{P}_i$$

has been maximized. For this purpose, a program has been written for the 709 IBM computer. From the distribution of the events as a function of position y in the chamber, Σ^+ production angle θ, and decay angle ϕ, the best values of the quantities b_0/a_0, c_0/a_0, and χ_b, χ_c were determined first. A preliminary analysis of the data indicated that all c.m. production angles could be accepted without any correction for experimental bias. Consequently, a and b have been set equal to -1 and $+1$, respectively, in Eq. (10). The parameter α has been assumed known. With the experimental data currently available from Σ-decay analysis taken into account,[16,17] and according to the discussion of Gell-Mann and Rosenfeld,[18] α^0 has been taken equal to $+1$ for events in which the Σ^+ decayed into $p+\pi^0$, and 0 for the $n+\pi^+$ decay mode. The likelihood function has been maximized for different values of $y_{\rm th}$ distributed in an interval where the threshold was thought to be. The absolute values of the amplitudes have then been computed from the mean cross section defined here by

$$\bar{\sigma}(\mathrm{mb}) = N/Knl, \quad (11)$$

where N = number of events produced by $\pi^+ p$ interactions in the chosen fiducial volume, limited by $y_{\rm min}$ and $y_{\rm max}$, n = total number of π^+ tracks entering the chamber through the thin window, counted at $y = y_{\rm min}$, l = track length per incident pion in the fiducial volume, and K = number of target protons per cm^3 of liquid hydrogen (0.35×10^{23}).

After substitution of Eqs. (3) and (6) into Eq. (1), integration over $\cos\theta$ and $\cos\phi$ gives

$$\sigma = 4\pi a_0^2 r(\Delta p)^{\frac{1}{2}} + 4\pi r^3[(2c_0^2+b_0^2)/3](\Delta p)^{\frac{3}{2}}. \quad (12)$$

Then the relation

$$\bar{\sigma} = \frac{\int_{y_{\rm min}}^{y_{\rm max}} \sigma \exp[-(y-y_{\rm min})/\lambda] dy}{y_{\rm max} - y_{\rm min}}, \quad (13)$$

with Δp (MeV/c) replaced by $0.243\times\Delta y$ (cm), allows the determination of the absolute amplitudes.

IV. EXPERIMENTAL RESULTS

In order to analyze experimental biases, the Σ^+ mean lifetime and decay branching ratio were determined.

A. Σ^+ Mean Lifetime

The mean lifetime of the Σ^+, $\bar{\tau}_{\Sigma^+}$, was obtained by the maximum-likelihood method. The likelihood function, maximized for various values of $t_{\rm min}$, reduces to

[16] R. L. Cool, B. Cork, J. W. Cronin, and W. A. Wenzel, Phys. Rev. **114**, 912 (1959); B. Cork, L. Kerth, W. A. Wenzel, J. W. Cronin, and R. L. Cool, *ibid.* **120**, 1000 (1960).

[17] E. F. Beall, Bruce Cork, D. Keefe, P. G. Murphy, and W. A. Wenzel, Phys. Rev. Letters **7**, 285 (1961).

[18] M. Gell-Mann and A. H. Rosenfeld, Ann. Rev. Nuclear Sci. **7**, 407 (1957).

TABLE I. Σ^+ lifetimes for various values of $t_{\min}$ for (a) $\Sigma^+ \to p+\pi^0$, and (b) $\Sigma^+ \to n+\pi$.

	N	$t_{\min}$ (10^{-10} sec)	$\bar{\tau}_{\Sigma^+}$ (10^{-10} sec)
(a)	104	0.50	$0.835_{-0.077}^{+0.088}$
	79	0.75	$0.810_{-0.090}^{+0.106}$
	56	1.00	$0.846_{-0.104}^{+0.124}$
(b)	192	0.25	$0.749_{-0.052}^{+0.056}$
	138	0.50	$0.749_{-0.060}^{+0.068}$
	103	0.75	$0.721_{-0.067}^{+0.076}$

the following expression when the potential time of flight for all events is large compared to $\bar{\tau}_{\Sigma^+}$:

$$\mathfrak{L}=\{\prod_{i=1}^{N}\exp[-(t_i-t_{\min})/\bar{\tau}_{\Sigma^+}]\}/\bar{\tau}_{\Sigma^+}{}^N, \qquad (14)$$

where t_i is the observed lifetime for the ith decay, N is the total number of decays for which $t_i>t_{\min}$, and $t_{\min}$ is some lower-limit cutoff below which one believes that the Σ^+ is sufficiently short to cause a bias. The decay modes $\Sigma^+ \to p+\pi^0$, and $\Sigma^+ \to n+\pi^+$ have been analyzed separately. The results of the analysis are given in Table I. In $\Sigma^+ \to p+\pi^0$ mode events in which the proton came off at less than 5 deg with the Σ^+ in the laboratory system, and events in which the Σ^+-p decay plane made an angle of less than 15 deg with the optic axes of the bubble chamber cameras have been excluded. The latter restriction removed events in which the Σ^+-p decay was nearly edge-on to the line of sight of the cameras. A fiducial volume limited by $-65\leqslant y\leqslant+51$ cm has been taken. The values obtained for both modes are in agreement with several other experiments.[4,19–21] A strong bias was observed (a) for $t_{\min}<0.50\times10^{-10}$ sec, and (b) for $t_{\min}<0.25\times10^{-10}$ sec.

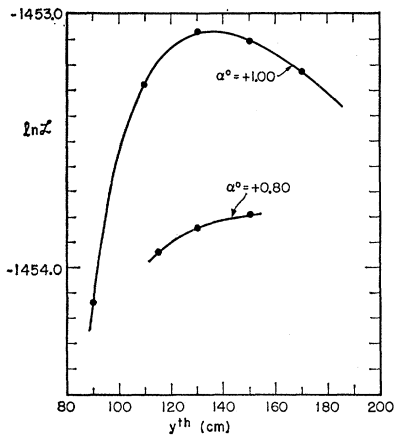

FIG. 1. Logarithm of the likelihood function vs y_{th} for $\alpha^0=+1.00$ and $\alpha^0=+0.80$.

[19] William E. Humphrey, Ph.D. thesis, Lawrence Radiation Laboratory Report UCRL-9752 (unpublished).

[20] D. A. Glaser, M. L. Good, and D. R. O. Morrison, in *Proceedings of the 1958 Annual International Conference of High-Energy Physics at CERN* (CERN Scientific Information Service, Geneva, 1958), p. 270.

[21] D. A. Glaser, in *Proceedings of the Ninth Annual International Conference on High-Energy Physics, Kiev, 1959* (Academy of Sciences, Moscow, 1960), p. 242.

B. Σ^+ Decay Branching Ratio

The 104 $\Sigma^+ \to p+\pi^0$ decays in Table I for which $t_i>0.50\times10^{-10}$ sec have been corrected for $t_i<0.50\times10^{-10}$ sec, using the corresponding calculated lifetime of 0.835×10^{-10} sec. The 5-deg decay cutoff and the 15-deg cutoff with the optic axes have been corrected, assuming that the Σ^+ decays in equal numbers forward and backward in its rest frame, and that in the laboratory system it decays uniformly with respect to its direction of motion. Based on the two scans, the scanning efficiency for $p\pi^0$ within the fiducial volume, and satisfying the above criteria, is $(95\pm5)\%$. These corrections give a total of 257 ± 31 events. The 192 $\Sigma^+ \to n+\pi^+$ decays need only be corrected for $t_i<0.25\times10^{-10}$ sec and a scanning efficiency of $(97\pm2)\%$. This gives 275 ± 21 events. Thus we have

$$\Sigma^+ \to p+\pi^0/(\Sigma^+ \to p+\pi^0)+(\Sigma^+ \to n+\pi^+) = 0.48\pm0.07. \qquad (15)$$

C. Average Cross Section

The average cross section for the energy interval defined by $-65\leqslant y\leqslant 51$ cm is given in Table II, along with other pertinent scanning information. The numbers of events have been corrected according to decay mode, in similar fashion to that done for the branching ratio calculation of the preceding section. All useful events were required to have their beam tracks pass through the bubble chamber thin window so that the resolution function mentioned previously would be applicable. No bias against events in which the Σ^+K^+ plane was edge-one with the cameras was observed.

D. *s*- and *p*-Wave Analysis

Preliminary analysis indicated that the threshold would be at $y=+130$ cm if the incident π^+ had continued in liquid hydrogen outside the chamber. This information was obtained by extrapolating the fitted beam-momentum distribution as a function of y at the rate 0.243 MeV/c per cm to the known threshold of 1020 MeV/c and, in addition, by extrapolation of the square of the average production angle of the K^+ as a function of y to the threshold by a curve of the form $(\theta^2)_{\text{av}}=\text{const}\times(y_{\text{th}}-y)$, as given by Wolf *et al.* for the reaction $\pi^-+p \to \Sigma^-+K^+$ near threshold.[8] These two methods provided consistent starting values in the search for the maximum-likelihood solution. A fiducial volume defined by -65 cm$\leqslant y\leqslant+51$ cm was taken; the beam was sufficiently collimated in the x and z directions (two dimensions normal to the beam direction) so that no cutoff was required. The results of the maximum-likelihood search are shown in Fig. 1. The natural logarithm of the likelihood function is maximum in the region $y_{\text{th}}=130$ to 135 cm. The fit has also been done with $\alpha^0=+0.80$. Figure 1 indicates that $+1.00$

TABLE II. Scanning information and mean cross section for the energy defined between $y_{\min} = -65$ cm and $y_{\max} = +51$ cm.

(a) Total number of pictures scanned	105526
(b) Total track length scanned (uncorrected)	$(1741.78 \pm 29.63) \times 10^3$ m
(c) Beam contamination	$(6.7 \pm 2.5)\%$
(d) Fraction of beam entering through bubble chamber thin window	0.96 ± 0.01
(e) Total π^+ track length, corrected for (c) and (d) above	$(1563.42 \pm 26.60) \times 10^3$ m
(f) Number of events with beam tracks entering bubble chamber through thin window (uncorrected)	274
(g) Scanning efficiency $\begin{Bmatrix} n\pi^+ \\ p\pi^0 \end{Bmatrix}$	$\begin{Bmatrix} (97 \pm 2)\% \\ (95 \pm 5)\% \end{Bmatrix}$
(h) Number of events with beam tracks entering through thin window, corrected for (g), lifetime, small-angle proton decay, and loss due to decay plane's being edge-on with cameras	364 ± 26
(i) Mean cross section ($\bar{\sigma}$)	0.067 ± 0.005 mb

is a better value of the asymmetry parameter. The maximum-likelihood solutions to the s- and p-wave parameters are given in Table III. Equation (3) shows that an alternative set of solutions exists for χ_b replaced by $-\chi_b$, and χ_c by $\pi - \chi_c$. The resultant amplitudes do not vary appreciably within their errors for this difference in the asymmetry parameter, nor with position of the threshold within the extreme values of Fig. 1. Because of the asymmetry of the resolution curve of the incident beam momentum, the mean value of the threshold is displaced to $\bar{y}_{\text{th}} = 122$ cm for a most probable value of $y_{\text{th}} = 130$ cm. Here $\bar{y}_{\text{th}} = 122 \pm 10$ cm has been taken as the best value of the threshold. The error on $\bar{y}_{\text{th}}$ is based primarily on the fitted-beam-momentum and K^+ angle extrapolation to the threshold. By use of the average cross section of Table II and Eq. (13), the square of the absolute amplitude a_0^2 has been computed. With the chosen values for $y_{\min}$ and $y_{\max}$ and $\bar{y}_{\text{th}} = 122$ cm, the expression

$$a_0^2\left(\frac{\text{mb}}{\text{sr}-\text{meV}/c}\right) = \bar{\sigma}(\text{mb})/$$

$$[1.30 \times 10^3 + 5.48(b_0^2/a_0^2 + 2c_0^2/a_0^2) \times 10^6], \quad (16)$$

gives $a_0^2 = (3.31 \pm 0.87) \times 10^{-5}$ mb/sr-MeV/c for the values of the parameters as given in Table III, with $\alpha^0 = +1.0$, and $y_{\text{th}} = 130.0$ cm.

With the information from Table III, the coefficients of Eq. (1) may be evaluated. Figure 2 shows the c.m. production angular distributions for Σ^+ given for the intervals (a) -65 cm $\leqslant y \leqslant +51$ cm, (b) -65 cm $\leqslant y \leqslant -7$ cm and (c) -7 cm $\leqslant y \leqslant +51$ cm. Curves (A) are calculated from Eq. (1-A) with the coefficients (Eq. 3) evaluated for the mean value of k corresponding to each energy interval. Curves (B) are the result of an independent maximum-likelihood fit to a second-order

TABLE III. Maximum-likelihood solutions to the s- and p-wave amplitudes for various values of α^0, y_{th}.

Parameters	$\alpha^0 = +1$, $y_{\text{th}} = 130$	$\alpha^0 = +1$, $y_{\text{th}} = 170$	$\alpha^0 = +0.8$, $y_{\text{th}} = 130$
b_0/a_0	0.0075 ± 0.0026	0.0080	0.0075
c_0/a_0	-0.0062 ± 0.0023	-0.0068	-0.0067
χ_b (deg)	52.1 ± 8.0	53.3	50.9
χ_c (deg)	80.8 ± 27.2	77.1	85.5

Error matrix ($\alpha^0 = +1$, $y_{\text{th}} = 130.0$ cm)

b_0/a_0	$+6.97 \times 10^{-6}$	-5.05×10^{-6}	$+1.13 \times 10^{-2}$	-2.54×10^{-2}
c_0/a_0		$+5.40 \times 10^{-6}$	-5.37×10^{-3}	$+2.49 \times 10^{-2}$
χ_b (deg)			+63.47	-43.78
χ_c (deg)				+740.10

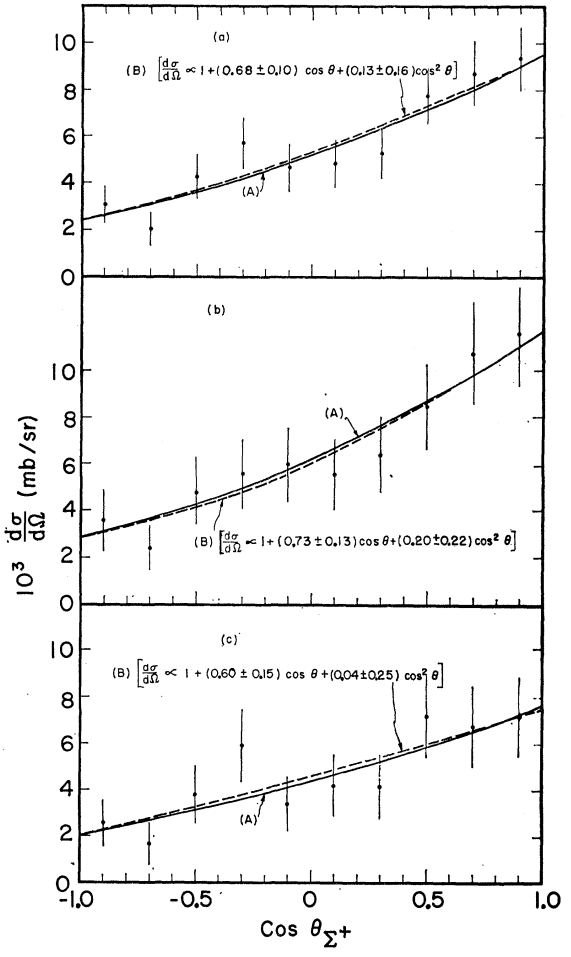

FIG. 2. Angular distributions for the different momentum intervals. The points have been determined from the observed number of events corrected for experimental biases and beam attenuation. The quoted errors are statistical.

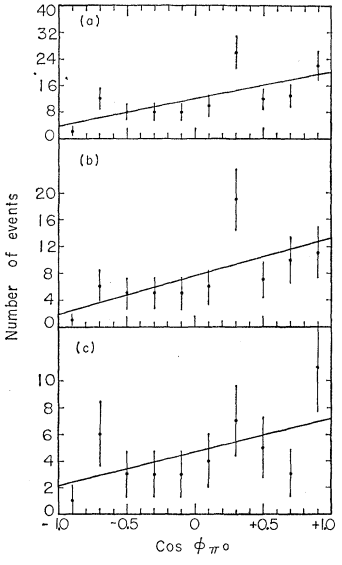

FIG. 3. Angular distributions of the decay pion with respect to the normal to the production plane for the $\Sigma^+ \to p+\pi^0$ mode. The quoted errors are statistical.

polynomial in $\cos\theta$. Curves (A) and (B) are consistent with each other in all cases. In order to compare the results of the fit with the observed polarization, the average polarization,

$$\bar{P}=\int_{-1}^{+1} P d\sigma^+ d\Omega d(\cos\theta) \Big/ \int_{-1}^{+1} d\sigma/d\Omega d(\cos\theta) = \frac{\pi}{4}\left[\frac{A_3}{(A_0+A_2/3)}\right], \quad (17)$$

has been computed, and is (a) +0.69, (b) +0.70, and (c) +0.66, for the three energy intervals given above. The experimental up-down distributions of the decay of the Σ^+ into $p+\pi^0$ are given in Fig. 3. The asymmetry coefficients for each of the energy intervals has been determined by a maximum-likelihood fit to the form $(1+\alpha^0\bar{P}\cos\phi)$; the results for $\alpha^0\bar{P}$ are (a) $=+0.68 \pm 0.14$, (b) $+0.76\pm0.18$, and (c) $+0.55\pm0.23$. The experimental up-down asymmetry of the Σ^+ into $n+\pi^+$ for -65 cm$\leqslant y \leqslant +51$ cm is given in Fig. 4. The maximum-likelihood fit to $(1+\alpha^+\bar{P}\cos\phi)$ gives $\alpha^+\bar{P}=+0.023\pm0.13$. If we use $\bar{P}\geqslant+0.68\pm0.14$ for

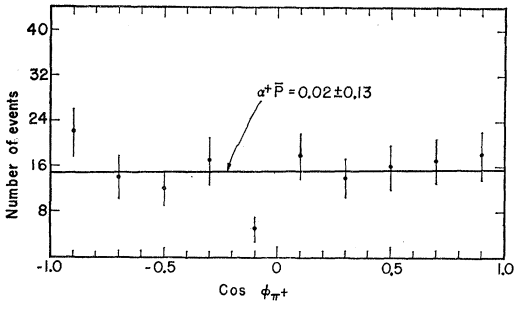

FIG. 4. Angular distribution of the decay pion with respect to the normal to the production plane for the $\Sigma^+ \to n+\pi^+$ mode. The quoted errors are statistical.

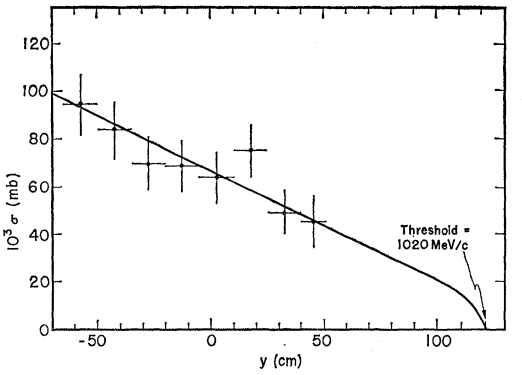

FIG. 5. Production cross section as a function of position in the chamber. The points have been determined from the observed number of events corrected for experimental biases and beam attenuation. The quoted errors are statistical. The solid curve has been computed from Eq. (18).

the corresponding energy interval from the $p\pi^0$ mode, then $\alpha^+ \leqslant 0.03\pm0.21$, which is in close agreement with the results of Cork *et al.*[16]

Lastly, the prediction of the maximum-likelihood solution with regard to the energy-excitation function has been considered. Upon use of the final solution of Table III, Eq. (12) becomes

$$\sigma(\text{mb})=0.00816(\Delta p)^{\frac{1}{2}}+0.000139(\Delta p)^{\frac{3}{2}}. \quad (18)$$

The distribution as a function of the production vertex y of the cross section computed from corrected numbers of events, and the path length corrected for beam attenuation, is shown in Fig. 5. The curve represents Eq. (18). Therefore the maximum-likelihood solutions of Table III are completely consistent with the c.m. production angular distribution, polarization, and the energy-excitation function. A summary of experimental results on Σ^+K^+ total cross sections and Σ^+ polarizations

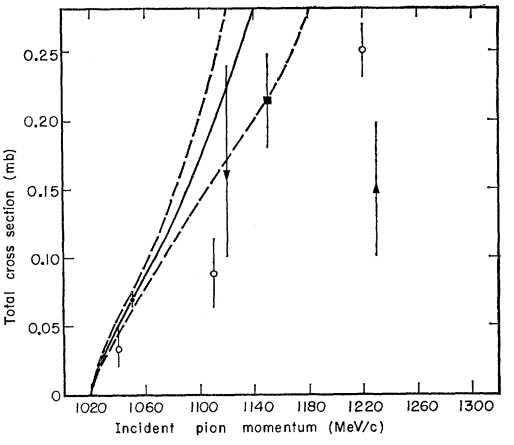

FIG. 6. The total cross section of this experiment compared with other experimental results. The solid curve has been determined from Eq. (18). The dashed curves represent one standard-deviation error, where proper account has been taken of correlations between errors. References to the data, cited from this article, are: (●) present experiment; (○) Baltay, reference 5; (■) Berthelot, reference 4; (▲) Brown, reference 1; and (▼) Erwin, reference 2.

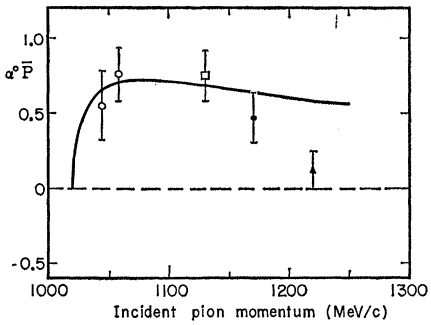

FIG. 7. The up-down asymmetries for the $\Sigma^+ \rightarrow p + \pi^0$ decay mode compared with other experimental results. The solid curve was determined from fitted s and p amplitudes. The result of Cool *et al.* has been determined by a counter experiment, looking at an angle (c.m.) of 87±15 deg. The corresponding value taken from s and p amplitudes is 0.92. Symbols are as follows: (●) from reference 23; (▲) from reference 5; (○) this experiment; (□) from reference 16.

is presented in Figs. 6 and 7, along with the prediction of the maximum-likelihood solution to s- and p-wave amplitudes. Deviation of the curves from the data beyond approximately 1150 MeV/c indicates that the energy dependence of the coefficients, represented by Eq. (3), is no longer valid at these energies. Nevertheless, in order to make a check of the charge-independence hypothesis,[22,23] the results of this analysis were extrapolated to 1090 MeV/c, where data of Σ^- and Σ^0 production by $\pi^- p$ interactions exists.[6,7] Based on this extrapolation, there is no evidence of a violation in either the total or differential cross sections.

ACKNOWLEDGMENTS

It is a pleasure to acknowledge Professor Frank S. Crawford, Jr., who generously placed films at the authors' disposal, and with whom many useful discussions were carried on in the course of the analysis. The authors also acknowledge the encouragement of Professor Luis W. Alvarez. Thanks go to J. Anderson and L. J. Lloyd for their aid in this experiment. One of us (F. G.) is grateful to the Institut Interuniversitaire des Sciences Nucléaires, Belgium, and to the U. S. Atomic Energy Commission for having made possible his stay at the Lawrence Radiation Laboratory, Berkeley.

[22] J. J. Sakurai, Phys. Rev. **107**, 908 (1957).
[23] G. A. Smith, F. Grard, and F. S. Crawford, Jr., Bull. Am. Phys. Soc. **7**, 297 (1962).

PHYSICAL REVIEW VOLUME 127, NUMBER 2 JULY 15, 1962

Electron-Proton Coincidences in Inelastic Electron-Deuteron Scattering*

M. CROISSIAUX†
High Energy Physics Laboratory, Stanford University, Stanford, California
(Received March 12, 1962)

Electron-proton coincidences in inelastic electron-deuteron scattering were detected under the following conditions: incident beam energy 500 MeV; electron scattered at 75° and 359 MeV; proton detected at 40° 23′ (the **q** direction for the e-p elastic scattering). The coincidence cross-section with a D_2 target was found to be $(4.2\pm0.8)\times10^{-32}$ cm²/sr² MeV. The experimental result agreed, within the statistical errors, with the value calculated from a theory of Durand. One may conclude that proton form factors in a bound state and the free state do not differ significantly.

I. INTRODUCTION

THE structure of nucleons and the nucleon-nucleon interaction are very important in modern physics. Durand[1] showed that the angular distribution of outgoing nucleons in inelastic electron-deuteron scattering can give much information on the nucleon form factors and the interaction between the nucleons in the final state of the neutron-proton system. To get such a distribution it is necessary to detect the scattered electron and the outgoing nucleon in coincidence. The presence of two magnetic spectrometers in the target room of the Stanford Mark III linear accelerator made possible such an experiment (or at least made it easier) by allowing the analysis in a precise way, of the momenta of two particles emitted simultaneously during a scattering experiment.

This article explains what kind of problems are encountered in the measurement of electron-proton coincidences from electron-deuteron collisions.[2] One of the objects of this experiment was to detect the coincidences; therefore, we chose the conditions such as to produce the largest number of coincidences. This means we placed the spectrometer for proton detection in the **q** direction, where **q** is the three-momentum transfer

* This work was supported in part by the Office of Naval Research and the U. S. Atomic Energy Commission and by the U. S. Air Force, through the Office of Scientific Research of the Air Research and Development Command.
† Now at the Centre de Recherches Nucléaires, Strasbourg, France.
[1] L. Durand, III, Phys. Rev. **115**, 1020 (1959).
[2] All details are in an internal report by M. Croissiaux, H.E.P.L., Stanford, 1962 (unpublished).